PHILOSOPHICAL TRANSACTIONS OF THE ROYAL SOCIETY A MATHEMATICAL, PHYSICAL & ENGINEERING SCIENCES

Radar Studies of High-Latitude Ionospheric Flows [and Discussion]

T. B. Jones, A. S. Rodger and K. J. Winser

Phil. Trans. R. Soc. Lond. A 1989 **328**, 107-118
doi: 10.1098/rsta.1989.0027

Phil. Trans. R. Soc. Lond. A **328**, 107–118 (1989)
Printed in Great Britain

Radar studies of high-latitude ionospheric flows

By T. B. Jones
Physics Department, University of Leicester, University Road, Leicester LE1 7RH, U.K.

Strong interactions occur between the solar wind and the Earth's magnetic field which result in the convection of ionospheric plasma over the polar cap regions. This generally forms a two-cell pattern with westward and eastward flows in the pre- and post-midnight sectors respectively. The flow pattern is sensitive to the flux of the solar wind and the direction of the interplanetary magnetic field. Observations of the flow pattern are thus of considerable value in the interpretation of the magneto-sphere–ionosphere coupling processes and in identifying the influence of the solar wind on the Earth's environment.

The plasma convection can be observed by ground-based coherent and incoherent scatter radars and the flow vectors determined. Measurements for a range of flow conditions are presented. These are interpreted in terms of the interactions of the solar wind with the magnetosphere and the resulting electric fields which drive the plasma flows in the ionosphere.

1. Introduction

Large-scale electric fields and their corresponding plasma convections are generated throughout the major part of the outer magnetosphere by dynamic coupling with the solar wind. The outer magnetosphere maps magnetically to the high-latitude regions of the Earth and the projection of the magnetospheric convection electric fields along geomagnetic field lines produce circulatory motions of plasma in the polar ionosphere. The charged particles move with the lines of force, provided the collision frequency is much less than the gyrofrequency. This condition ceases to be valid first for ions at a height of *ca.* 140 km, and then for electrons lower down at a height at *ca.* 80 km. Consequently in the E-region (100–110 km) large electric fields give rise to differential motion between the ions and the electrons and this constitutes a current.

The existence of ionospheric currents was originally inferred from the perturbations which they produce in the geomagnetic field measured at the ground, (Birkeland 1908; Chapman 1918). Chapman named these horizontal currents the auroral electrojets. Birkeland (1908) suggested that the electrojets are fed from outside the ionosphere by means of field-aligned currents (Birkeland currents) and direct experimental evidence for the existence of field-aligned currents in the polar region was provided by spacecraft observations of the distribution of field-aligned electron fluxes (Berko 1973; Berko *et al.* 1975) and by satellite magnetometer data (Zmuda *et al.* 1966; Armstrong & Zmuda 1970).

The diurnal variation of the geomagnetic field in the polar regions, may be attributed to a two-cell current system. Axford & Hines (1961) suggested that the magnetospheric flows are driven by 'viscous-like' interaction between the ionized material in the outer closed magnetosphere and the solar wind. Dungey (1961) proposed an alternative model which involves magnetic field-line reconnection on the magnetospheric boundary. Both these theories predict a twin-cell pattern of electron drift in the high latitude E-region, with a reversal of the

flow direction in the auroral zone near midnight (figure 1). The change in direction of the current flow was first noted by Harang (1946) in ground magnetometer data and this feature is now referred to as the Harang discontinuity (Heppner 1972). The high-latitude current system is generated by the coupling of the ionosphere to the solar-wind-driven magnetospheric flows by means of field-aligned currents (see, for example, Matsushita & Xu 1982) and is, thus, sensitive to changes in the solar wind, the magnetosphere and in the coupling mechanisms. In addition, this interaction can be influenced by the direction of the interplanetary magnetic field (IMF) (Akasofu *et al.* 1973).

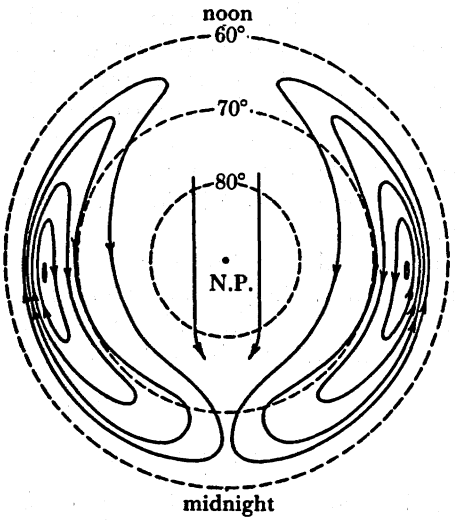

FIGURE 1. The symmetric two-cell ionospheric convection pattern predicted by the viscous interaction model. (From Axford & Hines 1961, N.P. is North Pole.)

Observations of the polar convection flows can provide a wealth of information concerning the coupling of the solar wind, magnetosphere and ionosphere. The flows and their temporal and spatial changes can be measured by ground-based radars, and some recent observations are presented and interpreted in terms of the ionosphere–magnetosphere coupling processes.

2. RADAR MEASUREMENTS OF CONVECTION FLOWS

Both coherent and incoherent radars can measure the high-latitude convection flows. In both types of radar the Doppler shift of the backscattered signal yields one component of the convection flow velocity. Incoherent radars require multistatic observations of a small common volume to determine the vector drift velocity. Alternatively, beam swinging techniques must be employed and assumptions made concerning the uniformity of the flow. In contrast, multistatic coherent radars can monitor a large spatial area with high spatial and temporal resolution. However, such measurements can only be made when the plasma irregularities necessary to produce the backscatter are present. All of the results presented in this paper have been obtained with coherent radars.

Radiowave backscatter can occur from field-aligned irregularities produced in the ionosphere by plasma instabilities. The most important of these are the two-stream and gradient drift instabilities (Farley 1963; Fejer *et al.* 1984).

PHILOSOPHICAL TRANSACTIONS OF THE ROYAL SOCIETY A MATHEMATICAL, PHYSICAL & ENGINEERING SCIENCES

The angular frequency of the plasma wave w can be written as

$$\omega = \boldsymbol{k}\cdot\boldsymbol{v}/(1+\psi), \quad \text{where} \quad \psi = (\nu_i \nu_e)/(\Omega_e \Omega_i).$$

$\boldsymbol{k}$ is the wave number and $\boldsymbol{v}$ the drift velocity. ν_i, ν_e and Ω_i, Ω_e are the ion and electron collison frequencies and gyrofrequencies respectively.

The growth rate γ of the instability is given as

$$\gamma = [\psi/(1+\psi)]\,(w^2 - k^2c^2)/\nu_i,$$

where c is the ion acoustic velocity.

The instabilities grow if $w^2 > k^2c^2$, i.e. when

$$(\boldsymbol{k}\cdot\boldsymbol{v})^2/(1+\psi)^2 > k^2c^2 \quad \text{and} \quad v\cos\theta > (1+\psi)\,c.$$

Because $\psi < 1$, the instabilities grow when the component of the velocity in the radar direction is greater than the ion acoustic velocity. The inclusion of plasma gradient effects can either increase or decrease the threshold value depending on the direction of the gradient. When the irregularities are illuminated by a radar pulse, Bragg-type backscatter will occur from those irregularities with spacing of half the radar wavelength. Maximum backscatter will be observed when the $\boldsymbol{k}$ vector of the radar is orthogonal to the field-line direction (figure 2). The range of plasma irregularity spacing is such that the backscatter can be detected over the entire frequency range from HF (5 MHz) to UHF (1 GHz) (ultra-high frequency).

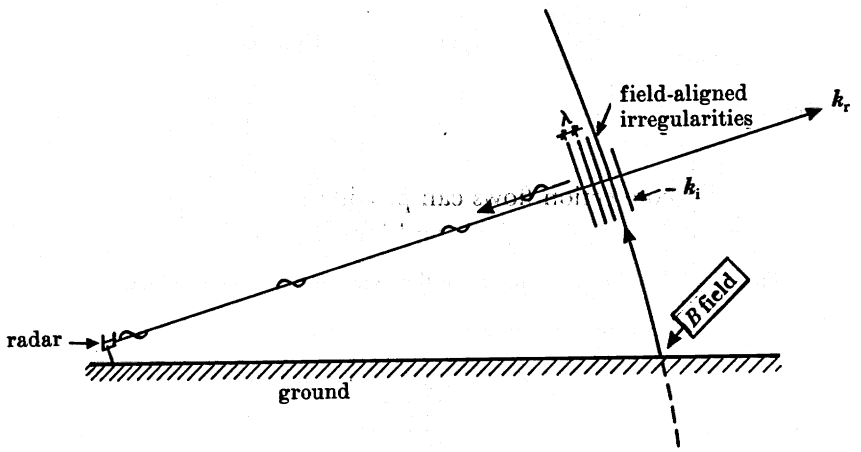

FIGURE 2. Schematic diagram of radar beam showing orthogonality to field-aligned irregularities and geometry of coherent radar observations. $2\boldsymbol{k}_r = \boldsymbol{k}_i$, $\boldsymbol{B}\cdot\boldsymbol{k}_r = 0$.

The above theory predicts that the field-aligned irregularities will move with the plasma drift velocity. Recent observations (Nielsen & Schlegel 1985) have indicated that the irregularities propagate at velocities which are lower than the plasma drift velocity. These observations can be accounted for by including nonlinear wave–particle effects in the above theory (Sudan 1983; Robinson 1986). This leads to a modified electron collision frequency which decreases the phase velocity of the plasma waves to a value close to the ion acoustic velocity. The measured Doppler frequency of the radar backscatter consequently underestimates the line-of-sight component of the plasma drift. However, the flow directions obtained from a bistatic system accurately represent the true plasma flow direction because of the geometrical factors involved.

PHILOSOPHICAL TRANSACTIONS OF THE ROYAL SOCIETY A MATHEMATICAL, PHYSICAL & ENGINEERING SCIENCES

3. The sabre radar

The Sweden and Britain Radar-auroral Experiment (SABRE) is a bistatic VHF auroral system with radars located at Wick in Scotland and Uppsala in Sweden. It was constructed jointly by Leicester University and the Max Planck Institute for Aeronomy, Lindau, and is operated in conjunction with the Ionospheric Institute at Uppsala. Each radar can observe along eight beam directions simultaneously and the 'look directions' are arranged to provide near field-line orthogonality in the viewing area (see figure 3). This area is approximately 200000 km^2

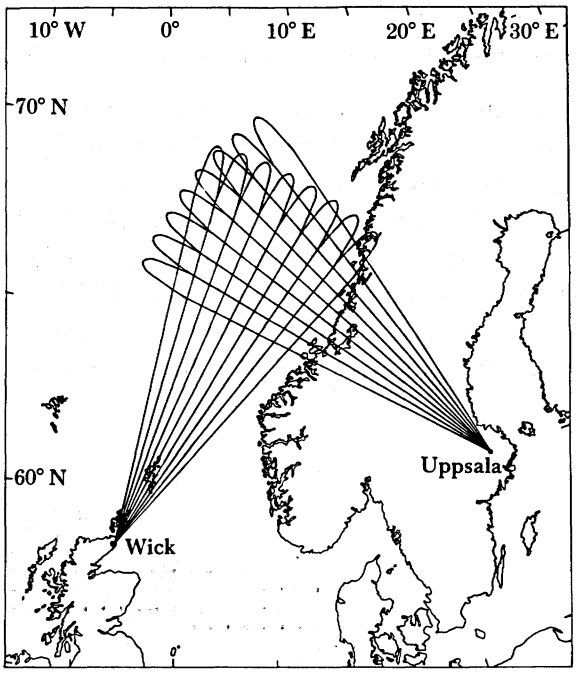

Figure 3. The beam geometry of the Wick and Uppsala radars.

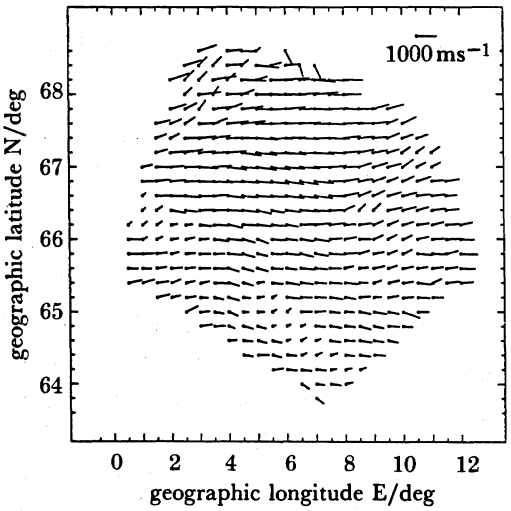

Figure 4. A typical example of the irregularity drift flows measured by SABRE as a function of geographic latitude and longitude and with a temporal resolution of 20 s. The observation is for 23h45 U.T., 28 October 1982 when SABRE viewed predominantly eastward flows associated with the westward electrojet.

in extent and within it a spatial resolution of 20×20 km^2 can be achieved. The temporal resolution is 20 s. The line-of-sight Doppler velocities from the two radars are merged to produce a vector velocity plot, an example of which is reproduced in figure 4. This illustrates the power of the technique to provide an instantaneous snapshot of the convection flow covering 10° in longitude and 6° in latitude with high spatial resolution. Recently a radar interferometer has been constructed at Wick which allows the height of the irregularities to be measured to ± 1 km (E. C. Thomas, personal communication 1988).

4. Regular flows

4.1. *The diurnal flow pattern*

The diurnal variation of the convection flows can readily be examined by the coherent radars. The velocity vectors measured by SABRE at various latitudes in a narrow longitudinal strip (100–102° geomagnetic long.) are plotted as a function of time in figure 5. As predicted

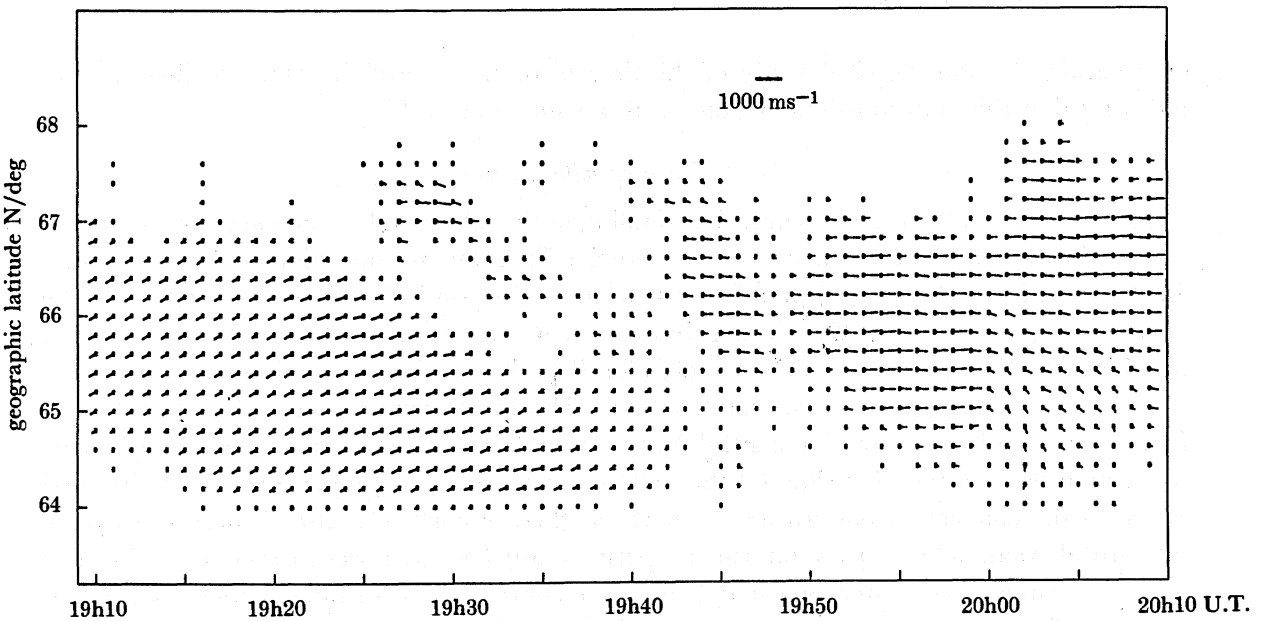

Figure 5. The convection pattern measured by SABRE as a function of Universal Time and geomagnetic latitude averaged over geomagnetic longitudes 100–102° E, showing the Harang discontinuity. (Day 261, 1982, averaged over 1 min in time and 5–7° E in geographic longitude.)

by the two-cell convection model, the flow reverses from westward to eastward as the radar viewing area corotates underneath the convection pattern in the afternoon and pre-midnight sector. The flow reversal at about 19h40 U.T. (universal time) is the Harang discontinuity. The detailed behaviour of the flow pattern varies from day to day, but the general features of figure 1, corresponding to a two-cell convection pattern, are generally present.

An important feature of the auroral zone is the equatorward expansion which occurs during periods of increased geomagnetic activity. Such an expansion would cause the flow reversals to occur at earlier times at a given observing location. This effect is clearly evident in figure 6, in which the average flow vectors are displayed according to the K_p value at the time of

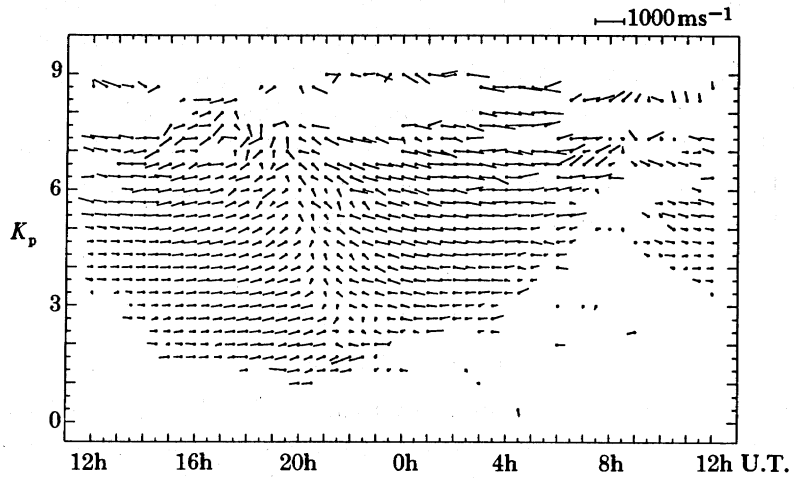

FIGURE 6. Mean convection flow velocities measured by SABRE, as a function of universal time and K_p, averaged over the geomagnetic latitude range 64.0–64.2° N and longitude 100–102° E. (Period of 1013 days from 22 March 1982 to 27 October 1986.)

observation. A more detailed study of the time of occurrence of the Harang discontinuity indicates that this is proportional to the local K value and to AE.

4.2. *Coupling with the IMF*

The direction of the IMF influences the coupling of the solar wind to the magnetosphere and this can be observed in the convection flow pattern. Field-line reconnection occurs more easily for southward IMF (B_z negative) than for northward IMF (B_z positive) and this is confirmed by the greater incidence of backscatter during times when B_z is negative. Little change is observed in the times of occurrence of the flow reversals for B_z both negative and positive.

The much closer dependence of the times of the Harang discontinuity on AE rather than on B_z suggests an indirect solar wind control, by means of the substorm processes, of the large-scale convection flow on the nightside. Of the three IMF components, B_z determines the latitudinal extent of the convection pattern and, hence, whether or not backscatter is observed by the subauroral SABRE radar. This is confirmed experimentally because the occurrence of backscatter is much greater during times when B_z is negative compared with similar periods when B_z is positive. The azimuthal component of IMF, B_y is found to exert a strong influence on the convection flow in the vicinity of the Harang discontinuity (see figure 7*a*, *b*). The flow reversals occur approximately one hour earlier for B_y positive. The two-cell structure is distorted when $B_y \neq 0$ and the form of the distortion varies according to whether B_y is negative or positive as shown schematically in figure 8. SABRE rarely observes polar cap flows and the occurence of B_y associated effects, thus, confirms the prediction of Cowley (1981) that B_y-associated asymmetries appear on closed (auroral zone) field lines as well as on open fields lines. The earlier occurrence of the flow reversal for B_y positive conditions is in agreement with the work of Cowley (1981) and Rodger *et al.* (1984); however, these observations are not consistent with the model proposed by Burch *et al.* (1985).

The influence of B_y in controlling the convection pattern can also be seen in the morning discontinuity (figure 9), although such events are only observed by SABRE during periods of high geomagnetic activity. The expected eastward flow is interrupted by a wedge of anomalous

PHILOSOPHICAL TRANSACTIONS OF THE ROYAL SOCIETY A MATHEMATICAL, PHYSICAL & ENGINEERING SCIENCES

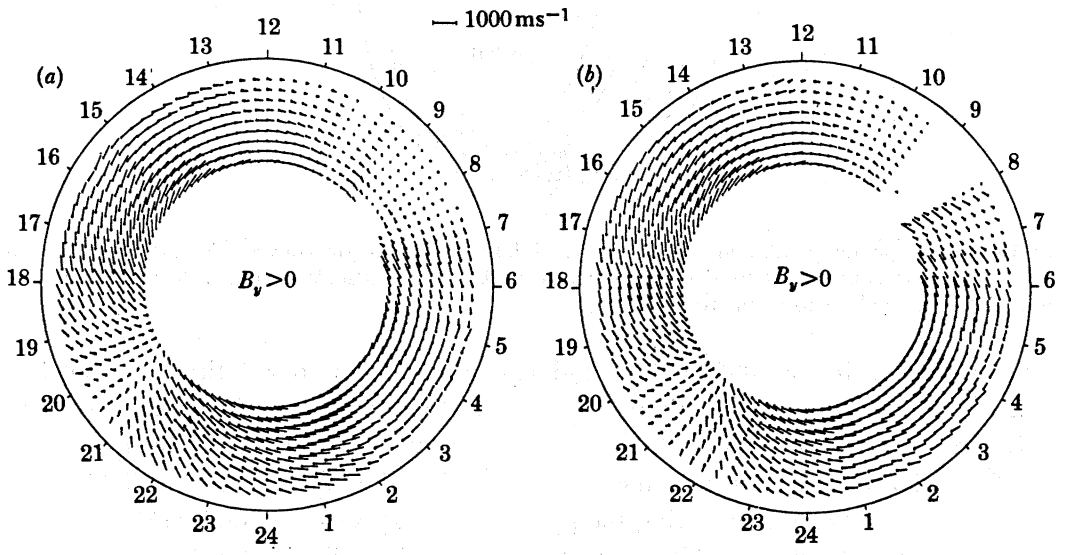

FIGURE 7. Mean convection flow velocities measured by SABRE as a function of geomagnetic latitude (62–66° N) and universal time (in hours) for (*a*) IMF $B_y < 0$ (*b*) IMF $B_y > 0$. (713 h of data for (*a*) and 783 h of data for (*b*). Both from 22 March 1982 to 22 March 1985.)

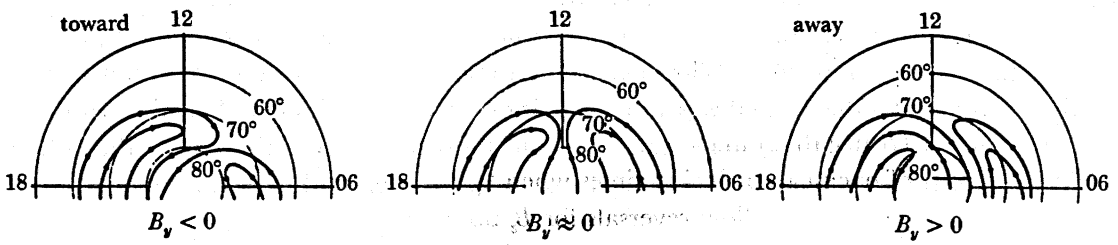

FIGURE 8. Schematic representation of the flow geometries in the dayside northern hemisphere, inferred from *AE-C* satellite observations, for different B_y conditions. B_z is negative and $|B_z|$ is constant in all cases. (From Heelis 1984.)

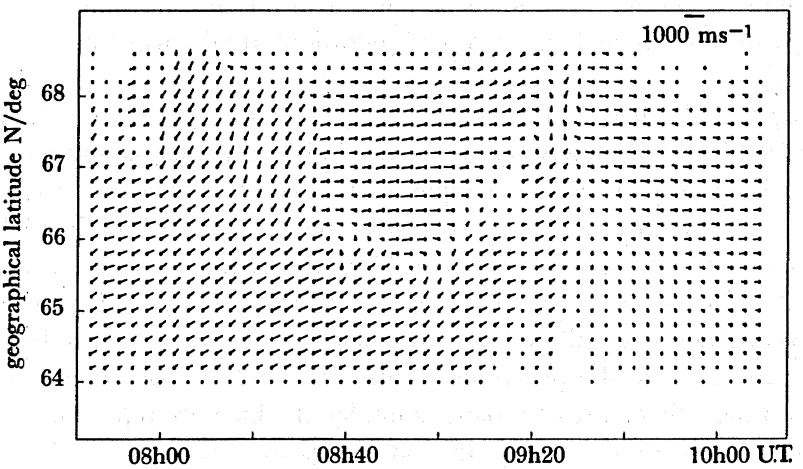

FIGURE 9. SABRE range-time-velocity (RTV) plot for the interval 07h45 to 10h15 U.T. (6 September 1982, day 249. Averaged over 3 min in time and 5–7° E in longitude.)

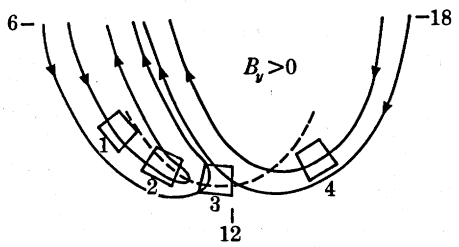

FIGURE 10. Schematic representation of the predicted large-scale dayside convection pattern for positive B_y indicating the successive positions of the SABRE viewing area as the Earth rotates under the pattern. The dashed line denotes the polar cap boundary.

westward flow starting at 08h35 U.T. and extending down to a latitude of 66° N. The westward flow is terminated at about 09h25 U.T. by a region of northeast directed flow which is associated with the main east–west flow reversal which subsequently occupies the whole extent of the viewing area. Measurements of the IMF by the *International Sun–Earth Explorer* 3 (*ISEE*-3) satellite indicate that during the period B_x and B_z were predominantly negative and that B_y was strongly positive. The average solar wind flow velocity was constant at approximately 600 km s^{-1}. The features of the measurements present in figure 9 can be accounted for in terms of an incursion of the polar cap flows into the SABRE viewing area. Figure 10 indicates schematically the movement of the SABRE viewing area through the discontinuity region. In position 1 only the normal eastward flows are observed. At position 2, the westward flows of the polar cap region are present at the northern extremity of the viewing area and produce the 'wedge' of westward flow extending to 66° N. The flows then turn northward at position 3 and finally the normal westward flow is observed at position 4. The observations are entirely consistent with this model and illustrate the excellent capabilities of the coherent radars (due to their high temporal and spatial resolution) for studies of this kind.

5. TRANSIENT CHANGES IN FLOW PATTERNS

The high spatial and temporal resolution of the coherent radars are ideal for studying transient changes in the convection flows. Such changes are associated with Pi2 and Pc5 pulsations (see Allan & Poulter 1984 for a review), field-line reconnection events and flow shears associated with field-aligned currents. Pc5 pulsations are discussed as examples of such transient disturbances.

Southwood (1974) and Chen & Hasegawa (1974) have suggested that these pulsations originate as a result of interaction between the solar wind and the magnetosphere through the Kelvin–Helmholtz instability at the magnetopause. This coupling gives rise to an evanescent wave between the magnetopause and the earth. Resonance occurs on field lines whose natural frequency of oscillation matches that of the wave. Thus, the frequency decreases as L increases, except when there are strong spatial gradients in the Alfvén velocity, which can occur at the plasmapause. This interaction modifies the electric fields which drive the instabilities required for auroral backscatter. Thus, the pulsation events can be clearly observed over the entire latitude range in a range–time–intensity plot, examples of which are reproduced in figure 11. A unique feature of these results is that the pulsations are observed moving in both the poleward (figure 11*a*) and equatorward (figure 11*b*) directions. Indeed, on many occasions the direction is seen to reverse during the course of the observation (figure 11*c*). The likely cause

PHILOSOPHICAL TRANSACTIONS OF THE ROYAL SOCIETY A MATHEMATICAL, PHYSICAL & ENGINEERING SCIENCES

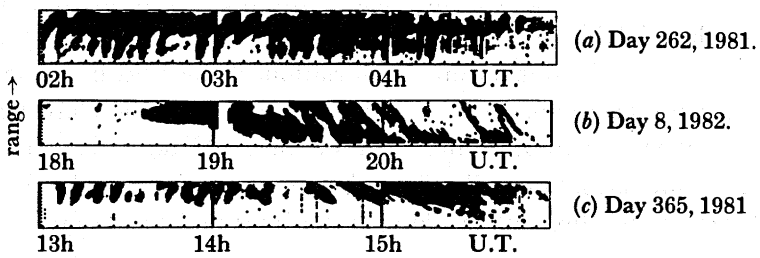

FIGURE 11. Range–time–intensity plots for a central beam of the Wick radar showing (*a*) poleward moving bands (*b*) equatorward moving bands and (*c*) an instance of reversal in the sense of phase motion.

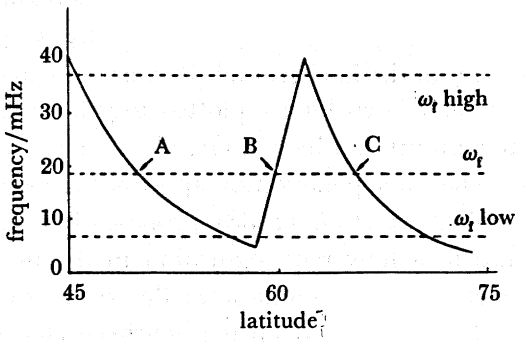

FIGURE 12. Illustrating the variation with latitude of the frequency of field-line resonance. For a given forcing frequency, resonance can occur at A, B or C (plasmasphere, plasmapause and plasmatrough, respectively). (From Orr & Hanson 1981.)

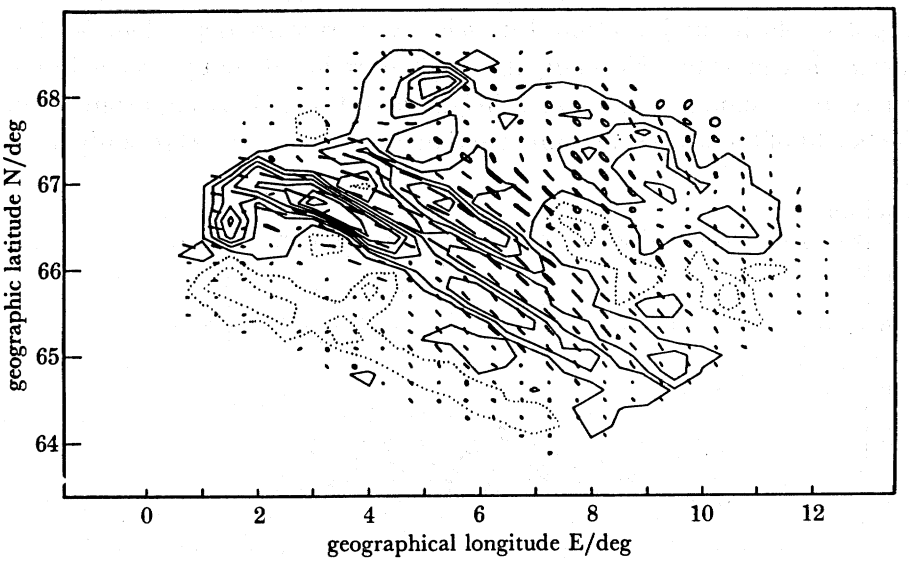

FIGURE 13. Polarization pattern derived from fast Fourier transform analysis of the SABRE data for the period 14h32 to 14h42 U.T. Superimposed is the field-aligned current pattern, averaged over the same period and estimated from the curl of the SABRE flow velocities. The full (dashed) contours represent an upward (downward) current.

PHILOSOPHICAL TRANSACTIONS OF THE ROYAL SOCIETY A MATHEMATICAL, PHYSICAL & ENGINEERING SCIENCES

of these changes appears to be connected with the variation in pulsation phase motion predicted by the Kelvin–Helmholtz theory. Orr & Hanson (1981) have shown that the plasmapause has a marked effect on the variation of the field-line resonance frequency as a function of L value (see figure 12). The radar results can therefore be accounted for if the plasmapause region moves into the field of view of the radar. The direction of phase propagation of the pulsation will then change according to the behaviour indicated in figure 12. From observations of this kind it becomes possible to investigate detailed features of the field-line resonances.

In a recent study Waldock *et al.* (1989) have described large-amplitude oscillatory signals in the Pc5 frequency band localized to a region of approximate dimension 300 km in the north–south direction and 100 km in the east–west direction. These waves are linearly polarized with an apparent westward horizontal phase speed of 8 km s^{-1}, and occur at a time when the background flow is changing temporally and spatially. In particular, the waves are collocated with a strong vorticity in the background flow, as indicated in figure 13, where the contours of the vertical component of curl $\boldsymbol{v}$ are plotted together with the wave polarization ellipses. The full and broken contours can be considered as the upward and downward field-aligned currents respectively. The wave polarization appears aligned along the direction of the field-aligned current sheet. Waldock *et al.* (1988) propose that the pulsations are system transients emitted in response to a flow reconfiguration in the magnetosphere, and this is supported by spacecraft observations of magnetospause flux transfer events (FTEs) occurring in the same local-time sector, although observed in the Southern Hemisphere.

6. Interferometry

Recent theoretical work (Robinson 1986) has indicated that the relation between the measured Doppler velocity and electron drift velocity is critically dependent on the height of the backscattering irregularities. Normally the coherent radars do not yield height information and the scatters are assumed to exist at a height of 110 km. It is important, therefore, to determine the height of the scattering sources and an interferometer has recently been installed

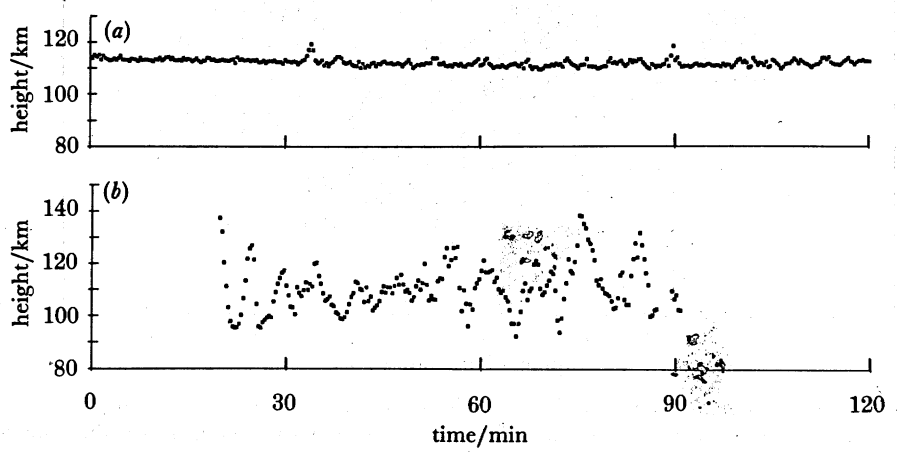

Figure 14. Interferometer measurements of the height of the backscattering irregularities. Typical examples are shown of (*a*) constant height conditions and (*b*) wave-like height changes. Data taken on (*a*) 25 September 1987, starting at 14h00 U.T. (range is 705 km); (*b*) 3 December 1987, starting at 15h00 U.T. (range is 930 km). Plot duration is 2 h for both.

at Wick which enables heights to be measured to an accuracy of ± 1 km. Figure 14 represents two distinct but typical examples of these observations. On 25 September 1987, scatter occurred at a height of 115 km which remained constant throughout the observing period. The behaviour on 3 December 1987 was completely different and there was a strong indication of wave-like features. These oscillations have a quasi-period of *ca.* 10 min and the height changes by ± 25 km. The cause of height changes has not yet been established but the presence of gravity waves, or of electric fields which modify the heights at which the scattering irregularities are produced, are possible mechanisms.

7. Summary

Coherent radar observations of the average auroral zone flow patterns and of transient disturbances in the flow have been presented. The features of the flow can be related to current models of ionosphere–magnetosphere–solar-wind coupling and a number of theoretical predictions have been verified by means of the radar observations. There is a growing interest in the plasma processes which generate the instabilities which give rise to the radar backscatter. Further development of the radars is necessary for these investigations since information such as the height of the irregularities and the spectral distribution of the backscattered signal is required. The coherent radar technique provides a powerful and cost-effective tool for both geophysics and plasma physics studies and the U.K. should continue to develop its expertise in this area.

References

Akasofu, S. I., Yasuhara, F. & Kawaski, K. 1973 *Planet. Space Sci.* **21**, 2232.
Allan, W. F. & Poulter, E. M. 1984 *Rev. Geophys. Space Phys.* **22**, 85.
Armstrong, J. C. & Zmuda, A. J. 1970 *J. geophys. Res.* **79**, 2501.
Axford, W. I. & Hines, C. O. 1961 *Can. J. Phys.* **39**, 1433.
Berko, F. W. 1973 *J. geophys. Res.* **78**, 1615.
Berko, F. W., Hoffman, R. A., Burton, R. K. & Holzer, R. E. 1975 *J. geophys. Res.* **80**, 37.
Birkeland, K. 1908 *Aschhloug Christiana*, **1**. Norway.
Burch, J. L., Reiff, P. H., Menietti, J. D., Heelis, R. A., Hanson, W. B., Shawhan, S. D., Shelley, E. C., Sugiura, M., Wiemer, D. R. & Winningham, J. D. 1985 *J. geophys. Res.* **90**, 1577.
Chapman, S. 1918 *Proc. R. Soc. Lond.* A**95**, 61.
Chen, L. & Hasegawa, A. 1974 *J. geophys. Res.* **79**, 1024.
Cowley, S. W. H. 1981 *Planet. Space Sci.* **29**, 79.
Dungey, J. W. 1961 *Phys. Rev. Lett.* **6**, 47–48.
Farley, D. T. 1963 *J. geophys. Res.* **68**, 5083.
Fejer, B. G., Providakes, J. & Farley, D. T. 1984 *J. geophys. Res.* **89**, 7487.
Harang, L. 1946 *J. geophys. Res.* **51**, 353.
Heelis, R. A. 1984 *J. geophys. Res.* **89**, 2873–2880.
Heppner, J. P. 1972 *Geophys. Pub.* **29**, 105.
Matsushita, S. & Xu, W. Y. 1982 *J. geophys. Res.* **87**, 8241.
Neilsen, E. & Schlegel, K. 1985 *J. geophys. Res.* **90**, 3498.
Orr, D. & Hanson, H. W. 1981 *J. atmos. terr. Phys.* **43**, 899.
Robinson, T. R. 1986 *J. atmos. terr. Phys.* **48**, 417.
Rodger, A. S., Cowley, S. W. H., Brown, M. J., Pinnock, M. & Simmons, D. 1984 *Planet. Space Sci.* **32**, 1021.
Southwood, D. J. 1974 *Planet. Space Sci.* **22**, 483.
Sudan, R. N. 1983 *J. geophys. Res.* **88**, 4853.
Waldock, J. A., Southwood, D. J., Freeman, M. P. & Lester, M. 1989 *J. geophys. Res.* (In the press.)
Zmuda, A. J., Martin, J. H. & Heuring, F. T. 1966 *J. geophys. Res.* **71**, 5033.

PHILOSOPHICAL TRANSACTIONS OF THE ROYAL SOCIETY A MATHEMATICAL, PHYSICAL & ENGINEERING SCIENCES

Discussion

A. S. RODGER (*British Antarctic Survey, Cambridge, U.K.*). It has been suggested in the literature that substorm activity is more prevalent for one direction of B_y compared with the other, for the same value of B_y. It was interesting to note that the noon day gap, when SABRE observes no backscatter returns owing to the low electric field within the receiving volume was *ca.* 1 h wide for B_y positive and *ca.* 3 h wide for B_y negative. Does Professor Jones attribute this difference in his data to a genuine geophysical difference or to an artefact of the relatively low sampling about these hours?

T. B. JONES. I doubt whether the effect Dr Rodger refers to is a genuine geophysical feature. In the dawn discontinuity region, the occurrence of backscatter in the SABRE radar viewing area is rather infrequent. The statistical significance of the observations during this period is therefore much less than that at other times of the day.

K. J. WINSER (*Rutherford Appleton Laboratory, Didcot, U.K.*). Dr Lockwood made an important point that the IMF B_x component can be an important factor in influencing the ionospheric convection pattern for different orientations of the IMF B_y and B_z components. Has this factor been studied by using SABRE or STARE data and, if so, have any marked effects been observed in convection flaws? (STARE is the Scandinavian twin auroral radar experiment.)

T. B. JONES. We have looked for effects associated with the change of direction of B_x. Unfortunately no features associated with this change are evident in our data. However, it might be worth reexamining the SABRE data in the light of the comments made at this meeting.

PHILOSOPHICAL TRANSACTIONS OF THE ROYAL SOCIETY A MATHEMATICAL, PHYSICAL & ENGINEERING SCIENCES